A Study of Viscoelastic Model of Polymers in Shear Flow Based on Molecular Dynamic Simulations

Donglei LIU [1, 2]**, Haizhen ZHOU** [1, 2]**, Kun FANG** [1, 2]**, Chuanliang CAO** [1] [*]

[1] *School of Mechanical and Electrical Engineering, Nanchang University, Nanchang, Jiangxi 330031, PR China*
[2] *Key Laboratory of Lightweight and High Strength Structural Materials of Jiangxi Province, Nanchang University, Nanchang, Jiangxi 330031, PR China*

In this study, the rheological properties and physical significations of an incompressible viscoelastic (inCVE) the inCVE model was investigated by employing molecular dynamics calculations. Polypropylene (PP) and polystyrene (PS) polymers were selected as candidate materials, the corresponding cell models consisting of five chains of 80 (PP) and 30 (PS) units were built successively. The energy minimization and anneal treatment were launched to optimize the unfavorable structures. The periodic boundary condition, COMPASS force field and the Velocity-Verlet algorithm were employed to calculate the shear flow behavior of chains. The sample data were collected and fitted based on the Matlab platform, and the analysis of the variance (ANOVA) method was performed to determine the validity of the model. Experimental results reveal that the inCVE model matches well with the pseudo-plastic fluids. Compared with the Ostwald-de Waele power law model and Cross model, it is effective and robust, and exhibits a three-stage rheological characteristic. Moreover, it characterizes the stress yield, activation energy, temperature dependence and viscoelastic response of polymers.
Keywords: shear flow, viscoelastic model, molecular dynamic simulation, thermoplastic polymer.

1. INTRODUCTION

Deformation and flow of sheared polymers are a fundamentally interesting and practically important issue in polymer science. Most of the polymer processing, such as coating, extrusion, spinning, and molding (rotation, compression or injection), is related to shear flows [1 – 4]. The shear flow of polymer melts is usually accompanied with the entanglement, orientation and time-temperature effects of macromolecular flexible chains, with obvious nonlinear characteristics. Usually, there are two approaches to describe the flow behavior of a rheologically complex fluid: phenomenological theory and molecular method.

In the first approach, numerous researches have been conducted to describe the rheological properties of polymers consisting of variation in viscosity with shear rates [5 – 9]. Owing to its simplicity and the small number of material parameters, the Ostwald-de Waele power law model, being made in phenomenological theory, was widely used in early polymer modeling fields, which can be used to mathematically express the power law region of a flow curve as follows [10]:

$$\eta = m\dot{\gamma}^{(n-1)}, \qquad (1)$$

where η is the viscosity; $\dot{\gamma}$ is the shear rate; m and n are the consistency constant and the power-law index, respectively. For polymer melts, the constant n lies between 0 and 1. The disadvantage of the Ostwald-de Waele power law model is that it does not correctly predict the zero-shear-rate viscosity at the low shear rate region.

The Carreau model and Cross model are other two preferred pure viscosity models in engineering applications, due to their ability to predict velocity and pressure distribution in uniform flows [11]. In comparing them on a variety of commercial-grade polymer melts, Hieber and Chiang found that the Cross model provides a better overall fit for the shear-rate dependence than that of the Carreau model [12]. The Cross model is shown as follows:

$$\eta = \frac{\eta_0}{1 + \left(\eta_0\dot{\gamma}/\tau^*\right)^{1-n}}, \qquad (2)$$

where η_0 is the viscosity at zero shear rate; τ^* is the shear stress at the transition between Newtonian and power law behavior. The Cross model combines a Newtonian region and a power law shear thinning region. Other types of the viscoelastic models including the Maxwell model [13], Oldroyd-B model [14], K-BKZ model [15] and the Leonov model [16] etc., have also been constructed to provide robust predictions in case of polymer materials.

In molecular method area, the FENE-P dumbbell model is an improvement on the Maxwell model based on the bead-spring method [17]. As another kinetic molecular theory, the Phan-Thien-Tanner (PTT) model has been derived based on network theory [18]. The eXtended Pom-Pom (XPP) model is the other simpler model based on the reputation theory [19]. These models can also predict the shear-thinning and first normal stress coefficient in dilute polymer solutions.

Efforts from previous researches, Liu et al. proposed a modest pseudo-high-elastic model to describe the

---

[*] Corresponding author. Tel.: +86-791-82969633.
E-mail address: *405529811@qq.com* (C. Cao)

instantaneous flow-induced orientation and stress response of polymer macromolecules with the incompressible and isothermal assumptions [20]. The model was studied based on the thermodynamics, statistical mechanics, and continuum mechanics using the molecular kinetic theory and the necessary simplification and hypothesis. Progressively, a feasible viscoelastic model was proposed to describe the shear flow behavior of thermoplastic polymers using the analogy method, which may be called incompressible viscoelastic (inCVE) model and can be simplified as the generalized Newton's law [21]. The integral formula of it is coincident with a special case of the K-BKZ model. The inCVE model was given by:

$$\tau = \frac{1}{2\pi\sqrt{2\pi}}\frac{3k_B T}{2nl^3}e^{-\frac{3}{2nl^2}}\left[\alpha_1 e^{\dot\gamma}(\dot\gamma - 3) + \alpha_2(\dot\gamma - \alpha_3)^2 + \alpha_4\right], \quad (3)$$

where τ represents the shear stress and $\dot\gamma$ represents the shear rate of the polymer element; k_B is the Boltzmann constant, the value of it is 1.38×10^{-23}J/K. T denotes the absolute temperature in thermodynamics, n is the number of links and l is the length of each link in a macromolecular chain, α_1, α_2, α_3 and α_4 are also constants of materials. This model contains the material's information including number of links and the length of link, etc., which is closely related to the viscoelastic properties of polymer.

Furthermore, the upper formula can be simplified as follows:

$$\tau = \frac{1}{2\pi\sqrt{2\pi}}\frac{3k_B T}{2nl^3}e^{-\frac{3}{2nl^2}}\left(\zeta_1\dot\gamma e^{\dot\gamma} + \zeta_2 e^{\dot\gamma} + \zeta_3\dot\gamma^2 + \zeta_4\dot\gamma + \zeta_5\right), (4)$$

where ζ_1-ζ_5 are constants.

As an alternative to the limitations of continuum-based approaches, molecular dynamics simulations have become as effective tool in analyzing the rheological behavior of the molecular level pattern transfer processes [22]. By adopting this method, Cui et al. [23] investigated the flow behaviors of nanofluids confined in nanochannel under different shear velocities. Xu at el. [24] studied the shear flow of rod-coil diblock copolymers in solutions by employing the nonequilibrium dissipative particle dynamics method. Kong et al. [25] studied the rheological properties of surfactant solutions by using dissipative particle dynamics algorithm too. Covind et al. [26] studied the effect of chain topology on the structural properties and diffusion of polymers in a dilute solution by using the molecular dynamics simulations, multiparticle collision dynamics and the lattice Boltzmann method. By adopting coarse-grained molecular dynamics simulation, Li et al. [27] investigated the effect of the chemical coupling between polymer and nanoparticles on the viscoelastic properties of polymer nanocomposites, Guo et al. [28] studied the effect of oscillatory shear strain amplitude on the viscoelastic behavior of nanorod filled polymer nanocomposites.

Ongoing previous studies, the aim of this paper is to present a better understanding of the rheological behavior of polymer in shear flow. For this purpose, the molecular dynamics simulations were launched by using PP and PS materials. The fitness and effectiveness of the inCVE

model was discussed by comparing with the Ostwald-de Waele power law model and Cross model. The physical signification of specific constants was also discussed. The scientific result may be helpful for potential industrial applications and benefits the users of certain plastic components.

2. EXPERIMENTAL DETAILS

To illustrate the scientific of the prepositional viscoelastic model, the isolated chains with degree of polymerization 80 of PP and 30 of PS were constructed separately. Then two of cubic cell boxes were generated with 5 monomer units successively. The initial density of the PP was set to be 0.89 g/cm^3 and the initial temperature was 298 K (25 ℃), while the initial density of another resin was set to be 1.05 g/cm^3 at the same initial temperature. The configurations of the simulated monomer, single chain and cell are given in Fig. 1, and the corresponding parameters of them are shown in Table 1.
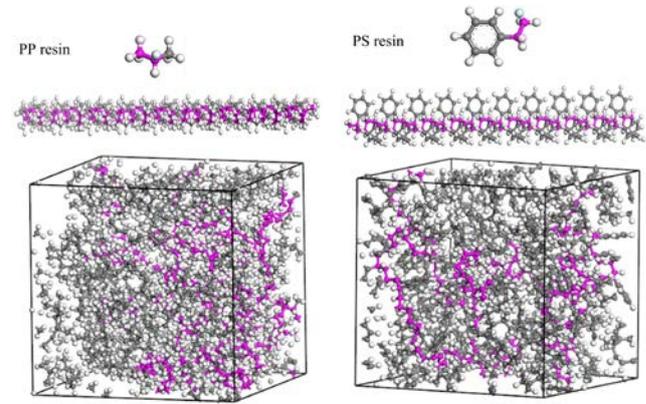
Fig. 1. Configurations of the monomer, chain and cell of resins

Table 1. Parameters of polymer models

Resins	PP	PS
Degree of polymerization	80	30
Number of chains	5	5
Length of monomer, nm	0.39	0.45
Number of atoms	3610	2410
Cell size, nm	3.156×3.156×3.156	2.913×2.913×2.913
Density, g/cm^3	0.89	1.05

In order to dispose of the unfavorable structures of models and get access to the actual processing conditions, energy minimization and anneal treatment have been done to optimize the molecular structure. In geometry optimization, the initial configurations were subject to 10,000 steps of energy minimization using the Smart method so as to reduce the magnitude of calculated forces and stresses. In annealing treatment, the temperature was increased and then decreased periodically 5 times from 300K to 500K to avoid trapping the structure in cells.

To simulate a macroscopic fluid, periodic boundary conditions were applied in three dimensions in order to eliminate surface effects. Molecular dynamics calculations were performed using the COMPASS (condensed-phase optimized molecular potentials for atomistic simulation studies) force field [29], and the Andersen algorithm was

used for temperature control [30]. Simulate method of Electrostatic was used Ewald, and a cutoff radius of 9.5 Å was applied to all the L-J interactions [31]. The motions of all atoms were resolved by means of the integration of Newton's second law of motion, using the so-called velocity Verlet algorithm [32].

During simulations, the dynamical relaxations were carried out firstly at specific temperature in the canonical NVT ensemble, i.e., at constant particle density and constant temperature, between 100,000 and 150,000 time steps firstly. Once the dynamical equilibrium was reached, the NVT thermostat was turned off and the simulation continued in the isothermal and isobaric conditions, NPT ensemble. During the NPT simulation, the shear stress was applied to the polymer cell in *x-y* plane, twenty-four different stresses were considered from 5 MPa to 120 MPa. The temperature of PP and PS were set at a range of 443 K – 463 K and 453 K – 483 K, respectively. The time step of 1fs was taken to be constant for all simulations, the steps of NPT MD simulations was 100000 (100 ps), and the output frequency was every 1000 steps.

In practices, the number of links *n* in Eq. 4 was represented as the account of monomers in cell, the length of link *l* was selected as the monomer length. The shear rate was calculated from the ratio of the displacement of polymer cell at specific shear time. The displacement spectrum was assumed to be well sampled when the chain has moved over a distance greater than its own end-to-end distance, which can be represented the mean square distance (MSD) of chains. That is:

$$\dot{\gamma} = \frac{MSD}{t} = \frac{\left\langle \left| r(t) - r(0) \right|^2 \right\rangle}{t}, \tag{4}$$

where *MSD* represents the mean square distance of chains. It is one of particular significance to assess their translation dynamics over broad time scales *t* [33]. *r*(t) and *r*(0) are the positions of the center of mass of chains at time t and 0, respectively. < > is the average of all the atoms in the cell.

3. RESULTS AND DISCUSSION

3.1. Rheological analysis

The comparison of the inCVE model and the Ostwald-de Waele power law model was fitted and depicted in Fig. 2. As shown in Fig. 2., all curves of the inCVE model can be characterized by three deformation stages: the first Newtonian stage, the viscoelastic yield stage and the second Newtonian area. This interesting phenomenon is more in line with the rheology properties of pseudo-plastic fluids, compared with the Ostwald-de Waele power law model. The simulation results also confirm the previous results of rheological experiments. All curves of the inCVE model, whether PP or PS resins, show quasi-linear increasing tendency in primary stage, turn into a slight growth trend after reaching a peak value in middle stage, and then give another dramatic increasing trendy finally.

Specifically, the shear rate of the inCVE model to PP reaches to the first peak value about 6890 s^{-1} of 453 K and 50 MPa, 6120 s^{-1} of 463 K and 45 MPa, 5900 s^{-1} of 473 K and 45 MPa, respectively. While it reaches to another

inflection point about 13800 s^{-1} of 453 K and 60 MPa, 9800 s^{-1} of 463 K and 55 MPa, 12100 s^{-1} of 473 K and 60 MPa, successively. For PS, the first inflection point of curves about the inCVE model appears around 4900 s^{-1} of 453 K and 60 MPa, 5500 s^{-1} of 463 K and 65 MPa, 5500 s^{-1} of 473 K and 65 MPa, 4700 s^{-1} of 483 K and 60 Pa, repressively.

a

b
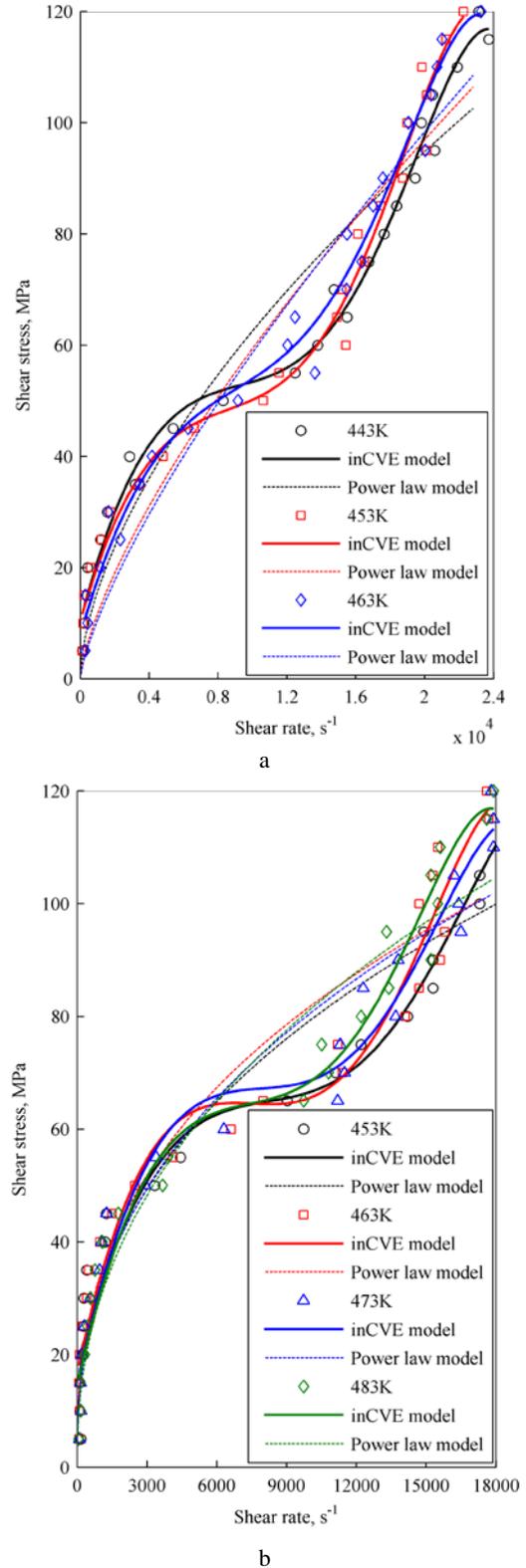
Fig. 2. The inCVE model versus the Ostwald-de Waele power law model: a – PP; b – PS

While the second inflection point appears about 8400 s^{-1} of 453 K and 65 MPa, 10800 s^{-1} of 463 K and 65 MPa, 10500 s^{-1} of 473 K and 65 MPa, 8000 s^{-1} of 483 K and 65 MPa, repressively.

Furthermore, the fitness of these models can also be evaluated by calculating the analysis of variance (ANOVA), as shown in Table 2 and Table 3, where *SSE*, *RMSE*, *R*-square (R^2) and Adjusted *R*-square (R^2_{adj}) represent the sum of square due to error, root mean squared error, coefficient of determination and degree-of-freedom adjusted coefficient of determination, respectively. Compared with the Ostwald-de Waele power law model, *SSE* and *RMSE* values of the inCVE model is smaller, and R^2 and R^2_{adj} values of it is bigger, which illustrates the speculative inCVE model has a better consistency with the actual shear behavior than the classical model.

Table 2. ANOVA results of different models (PP)

Models	Constants	Temperature, K		
		443	453	463
inCVE model	*SSE*	286	419.9	436.7
	RMSE	3.88	4.701	4.794
	R^2	0.990	0.985	0.985
	R^2_{adj}	0.988	0.982	0.982
Power law model	*SSE*	2109	2341	1944
	RMSE	9.79	10.31	9.401
	R^2	0.923	0.917	0.932
	R^2_{adj}	0.923	0.915	0.929
Cross model	*SSE*	2111	2409	2004
	RMSE	0.927	10.71	9.769
	R^2	0.920	0.916	0.930
	R^2_{adj}	10.03	0.9082	0.924

Table 3. ANOVA results of different models (PS)

Model	Constants	Temperature, K			
		453	463	473	483
inCVE model	*SSE*	861.3	1060	846.3	750.7
	RMSE	6.73	7.47	6.67	6.29
	R^2	0.97	0.963	0.971	0.974
	R^2_{adj}	0.964	0.955	0.964	0.968
Power law model	*SSE*	1940	2028	1854	1696
	RMSE	9.39	9.602	9.181	8.781
	R^2	0.933	0.930	0.937	0.941
	R^2_{adj}	0.930	0.926	0.933	0.938
Cross model	*SSE*	1940	2028	1854	1696
	RMSE	9.611	9.828	9.397	8.988
	R^2	0.933	0.930	0.936	0.941
	R^2_{adj}	0.926	0.923	0.929	0.935

Fig. 3 gives the fitted results of the inCVE model and Cross model. Accordingly, the ANOVA results of them are also illustrated in Table 2 and Table 3. It can be seen from Fig. 3. that the inVCE model matches well with the rheological practices within the current test window. The ANOVA results further confirm that the inCVE model exhibits a better consistency than that of the Cross model.

3.2. Physical signification of constants

The constants of the inCVE model and others were calculated and listed in Table 4 and Table 5. As can be seen from Tables that all terms of the inCVE model's constants are positive, with the exception of the second

term ζ_2. It corresponds to the exponential term, and is just coincident with the Arrhenius formula.
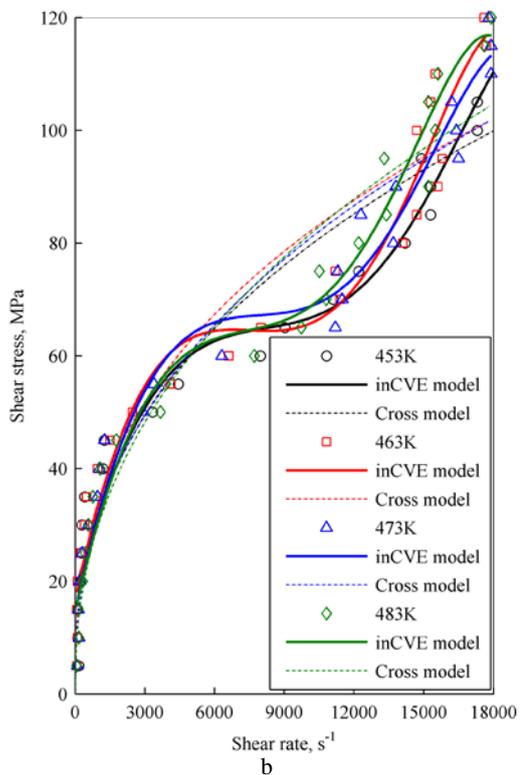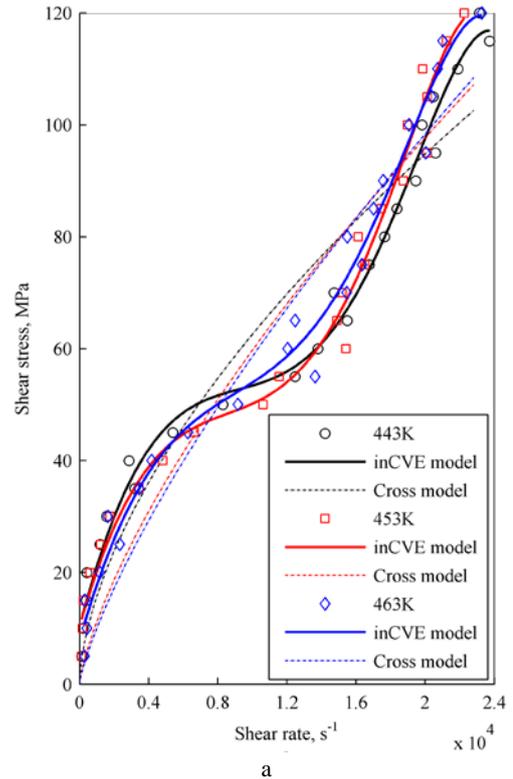
Fig. 3. The inCVE model versus the Cross model: a – PP; b – PS

This indicates that the inCVE model contains the activation energy information of materials, which hinders the movement of polymer macromolecules and therefore appears to be negative in form. That is to say, there is an initial energy barrier before macromolecules movement in shear flow. Actually, it's not difficult to understand this

phenomenon at molecular-level. The static polymer chain needs first to overcome the intermolecular forces, the kink forces and the internal frictions effect from the surrounding macromolecules. Only the shear stress increases to a plenty high enough, will the migration phenomena of them begin to undergo and become apparent.

Table 4. Constants of different models (PP)

Models	Constants	Temperature, K		
		443	453	463
inCVE model	ζ_1	0.09	0.07	0.05
	ζ_2	−0.31	−0.25	−0.19
	ζ_3	0.06	0.05	0.04
	ζ_4	0.22	0.17	0.13
	ζ_5	0.30	0.24	0.17
Power law model	m	0.25	0.09	0.06
	n	0.60	0.71	0.75
Cross model	η_0	2.83	0.05	0.03
	τ^*	0.25	0.13	0.11
	n	0.60	0.69	0.72

Table 5. Constants of different models (PS)

Models	Constants	Temperature, K			
		453	463	473	483
inCVE model	ζ_1	0.14	0.17	0.16	0.14
	ζ_2	−0.50	−0.61	−0.56	−0.49
	ζ_3	0.11	0.13	0.12	0.11
	ζ_4	0.36	0.44	0.41	0.35
	ζ_5	0.47	0.58	0.53	0.46
Power law model	m	2.11	2.50	1.95	1.5
	n	0.39	0.38	0.40	0.43
Cross model	η_0	$2.31*10^4$	$2.16*10^4$	$1.56*10^4$	$1.84*10^4$
	τ^*	2.11	2.50	1.96	1.51
	n	0.39	0.38	0.40	0.43

It can also be found from Fig. 2 and Fig. 3 that there is a non-zone stress startup point of the inCVE model, different from others. In retrospect now, it is understandable that there is a constant term in the inCVE model, i.e., ζ_5. The fitted result of it is always not equal to zero, as shown in Table 3. The interesting phenomenon indicates that there is an extrapolation length in velocity fields in shear flow, which needs additional kinetic energy to overcome the potential resistance for motion in startup stage. That is to say, there is a stress yield before the deformation or stretching occurs under the shear loaded condition. As we know, temperature dependence of the Ostwald-de Waele power law model is usually included by multiplying the formula by an exponential term [34]. Further analysis found that the first item in the inCVM model is also the shear rate multiplied by its exponential term. From this perspective, the first constant ζ_1 of the inCVE model characterizes the temperature-dependent constant. While the constants of the quadratic and linear term, i.e., ζ_3 and ζ_4, are relevant to the viscoelastic relaxation response of polymer materials.

4. CONCLUSIONS

In this paper, molecular dynamics simulations were conducted to investigate the rheological property and physical signification of the inCVE model. The PP and PS polymers were selected as candidate materials. The macromolecules models consisting of five chains of 80 (PP) and 30 (PS) monomers were constructed successively. The energy minimization and anneal treatment were launched to optimize the unfavorable structures. The periodic boundary condition was imposed to eliminate surface effects of models. COMPASS force field and Velocity-Verlet algorithm were employed to simulate the shear flow behavior of macromolecules. Experimental results reveal the inCVE model matches well with the shear flow behavior of pseudo-plastic fluids. It shows a obvious three-stage rheological behavior, and exhibits a better consistency than that of the Ostwald-de Waele power law model and Cross model. The inCVE model contains the material information, such as the stress yield, activation energy, temperature dependence and viscoelastic response parameters, etc.. The scientific result is helpful for studying the shear theological behavior of polymers.

REFERENCES

1. **Li, J., Nie, Y.J., Ma, Y., Hu, W.B.** Stress-induced Polymer Deformation in Shear Flows *Chinese Journal of Polymer Science* 31 (11) 2013: pp. 1590 – 1598. https://doi.org/10.1007/s10118-013-1354-0
2. **Balasubramanian, V., Denniston, C.** Polymer Margination in *Uniform* Shear Flows *Soft Matter* 45 (14) 2018: pp. 9209 – 9219. https://doi.org/10.1039/C8SM01445K
3. **Luo, F., Liu, X., Shao, C., Zhang, J., Shen, C., Guo, Z.** Micromechanical Analysis of Molecular Orientation in High-temperature Creep of Polycarbonate *Materials & Design* 144 2018: pp. 25 – 31. https://doi.org/10.1016/j.matdes.2018.02.025
4. **Zhang, Y., Yu, W., Liang, J., Lang, J., Li, D.** Three-dimensional Numerical Simulation for Plastic Injection-Compression Molding *Frontiers of Mechanical Engineering* 13 (5) 2018: pp. 74 – 84. https://doi.org/10.1007/s11465-018-0490-1
5. **Campbell, G.A., Zak, M.E., Wetzel, M.D.** Newtonian, Power Law, and Infinite Shear Flow Characteristics of Concentrated Slurries Using Percolation Theory Concept *Rheologica Acta* 57 2018: pp. 197 – 216. https://doi.org/10.1007/s00397-017-1070-8
6. **Aho, J., Ayrjala, S.** Shear Viscosity Measurements of Polymer Melts Using Injection Molding Machine with Adjustable Slit Die *Polymer Testing* 30 (6) 2011: pp. 595 – 601. https://doi.org/10.1016/j.polymertesting.2011.04.014
7. **Razavi, A., Shirani, E., Sadeghi, M.R.** Numerical Simulation of Blood Pulsatileflow in a Stenosed Carotid Artery Using Different Rheological Models *Journal of Biomechanics* 44 2011: pp. 2021 – 2030. https://doi.org/10.1016/j.jbiomech.2011.04.023
8. **Munstedt, H.** Rheological of Rubber-modified Polymer Melts *Polymer Engineering and Science* 21 (5) 2010: pp. 259 – 270. https://doi.org/10.1002/pen.760210503
9. **Huang, J., Lu, X., Zhang, G., Qu, J.** Study on the

Rheological, Thermal and Mechanical Properties of Thermoplastic Polyurethane/poly (Butylene Terephthalate) Blends *Polymer Testing* 36 2014: pp. 69–74. https://doi.org/10.1016/j.polymertesting.2014.03.006

10. **Werner, F., Mersmann, A.** About the Rheology of Polymer Solutions; Part 2: A Model for the Prediction of the Concentration Dependence of the Rheological Parameters of Power-law Fluids *Chemical Engineering & Technology* 21 (8) 1998: pp. 644–647. https://doi.org/10.1002/(SICI)1521-4125(199808)21:8<644::AID-CEAT644>3.0.CO;2-1

11. **Drabek, J., Zatloukal, M., Martyn, M.** Effect of Molecular Weight on Secondary Newtonian Plateau at High Shear Rates for Linear Isotactic Melt Blown Polypropylenes *Journal of Non-Newtonian Fluid Mechanics* 251 2018: pp. 107–118. https://doi.org/10.1016/j.jnnfm.2017.11.009

12. **Hieber, C.A., Chiang, H.H.** Shear-rate-dependence Modeling of Polymer Melts Viscosity *Polymer Engineering & Science* 32 (14) 1992: pp. 931–938. https://doi.org/10.1002/pen.760321404

13. **Bird, R.B., Wiest, J.M.** Constitutive Equations for Polymeric Liquids *Annual Review of Fluid Mechanics* 27 (1) 1995: pp. 169–193. https://doi.org/10.1146/annurev.fl.27.010195.001125

14. **Barrett, J.W., Boyaval, S.** Existence and Approximation of a (regularized) Oldroyd-B Model *Mathematical Models and Methods in Applied Sciences* 21 (9) 2011: pp. 1783–1837. https://doi.org/10.1142/S0218202511005581

15. **Tanner, R.I.** From A to (BK) Z in Constitutive Relations *Journal of Rheology* 32 (7) 1988: pp. 673–702. https://doi.org/10.1122/1.549986

16. **Maders, H., Vergnes, B., Demay, Y., Agassant, J.F.** Steady Flow of a White-Metzner Fluid in a 2-D Abrupt Contraction: Computation and Experiments *Journal of Non-Newtonian Fluid Mechanics* 45 (1) 1992: pp. 63–80. https://doi.org/10.1016/0377-0257(92)80061-2

17. **Bird, R.B., Dotson, P.J., Johnson, N.L.** Polymer Solution Rheology Based on a Finitely Extensible Bead-Spring Chain Model *Journal of Non-Newtonian Fluid Mechanics* 7 (2–3) 1980: pp. 213–235. https://doi.org/10.1016/0377-0257(80)85007-5

18. **Thien, N.P., Tanner, R.I.** A New Constitutive Equation Derived from Network Theory *Journal of Non-Newtonian Fluid Mechanics* 2 (4) 1977: pp. 353–365. https://doi.org/10.1016/0377-0257(77)80021-9

19. **Verbeeten, W.M., Peters, G.W., Baaijens, F.P.** Differential Constitutive Equations for Polymer Melts: The Extended Pom-Pom Model *Journal of Rheology* 45 (4) 2001: pp. 823–843. https://doi.org/10.1122/1.1380426

20. **Liu, D.L., Cao, W., Xin, Y., Sun, L.** Relationship Model Theory of Polymer Orientation Stress-morphology for Incompressible and Isothermal Melts in Injection Molding *Polymeric Materials Science and Engineering* 30 (8) 2014: pp. 109–118. https://doi.org/10.16865/j.cnki.1000-7555.2014.08.022

21. **Liu, D., Fang, K.** A Study of the Transient Shear Flow Behavior of the Incompressible and Isothermal Thermoplastic Polymer Materials *Advances in Mechanical Engineering* 11 (5) 2019: pp. 1–9. https://doi.org/10.1177/1687814019852829

22. **Li, Y., Xu, J., Li, D.** Molecular Dynamics Simulation of Nanoscale Liquid Flows *Microfluidics & Nanofluidics*

9 (6) 2010: pp. 1011–1031. https://doi.org/10.1007/s10404-010-0612-5

23. **Cui, W., Shen, Z., Yang, J., Wu, S.** Molecular Dynamics Simulation on Flow Behaviors of Nanofluids Confined in Nanochannel *Case Studies in Thermal Engineering* 5 2015: pp. 114–121. https://doi.org/10.1016/j.csite.2015.03.007

24. **Xu, P., Lin, J., Wang, L., Zhang, L.** Shear Flow Behaviors of Rod-coil Diblock Copolymers in Solution: A Nonequilibrium Dissipative Particle Dynamics Simulation *The Journal of Chemical Physics* 146 (18) 2017: pp. 184903. https://doi.org/10.1063/1.4982938

25. **Kong, Y., Manke, C.W., Madden, W.G., Schlijper, A.G.** Modeling the Rheology of Polymer Solutions by Dissipative Particle Dynamics *Tribology Letters* 3 (1) 1997: pp. 133–138. https://doi.org/10.1023/A:1019196014223

26. **Hegde, G.A., Chang, J.F., Chen, Y.L., Khare, R.** Conformation and Diffusion Behavior of Ring Polymers in Solution: A Comparison between Molecular Dynamics, Multiparticle Collision Dynamics, and Lattice Boltzmann Simulations *The Journal of Chemical Physics* 135 (18) 2011: pp. 184901. https://doi.org/10.1063/1.3656761

27. **Li, Z., Liu, J., Zhang, Z., Gao, Y., Liu, L., Zhang, L., Yuan, B.** Molecular Dynamics Simulation of the Viscoelasticity of Polymer Nanocomposites under Oscillatory Shear: Effect of Interfacial Chemical Coupling *RSC Advances* 8 (15) 2018: pp. 8141–8151. https://doi.org/10.1039/C7RA13415K

28. **Gao, Y., Hu, F., Wu, Y., Liu, J., Zhang, L.** Understanding the Structural Evolution under the Oscillatory Shear Field to Determine the Viscoelastic Behavior of Nanorod Filled Polymer Nanocomposites *Computational Materials Science* 142 2018: pp. 192–199. https://doi.org/10.1016/j.commatsci.2017.09.051

29. **Sun, H.** COMPASS: An ab initio Force-field Optimized for Condensed-phase Applications Overview with Details on Alkane and Benzene Compounds *The Journal of Physical Chemistry B* 102 (38) 1998: pp. 7338–7364. https://doi.org/10.1021/jp980939v

30. **Andersen, H.C.** Molecular Dynamics Simulations at Constant Pressure and/or Temperature *The Journal of Chemical Physics* 72 (4) 1980: pp. 2384–2393. https://doi.org/10.1063/1.439486

31. **Zhou, M., Jiang, B., Weng, C.** Molecular Dynamics Study on Polymer Filling into Nano-cavity by Injection Molding *Computational Materials Science* 120 2016: pp. 36–42. https://doi.org/10.1016/j.commatsci.2016.04.004

32. **Martys, N.S., Mountain, R.D.** Velocity Verlet Algorithm for Dissipative-particle-dynamics-based Models of Suspensions *Physical Review E* 59 (3) 1999: pp. 3733. https://doi.org/10.1103/PhysRevE.59.3733

33. **Saha, S., Bhowmick, A.K.** An Insight into Molecular Structure and Properties of Flexible Amorphous Polymers: A Molecular Dynamics Simulation Approach *Journal of Applied Polymer Science* 136 (18) 2019: pp. 47457. https://doi.org/10.1002/app.47457

34. **Shapovalov, V.M.** On the Applicability of the Ostwald–De Waele Model in Solving Applied Problems *Journal of Engineering Physics and Thermophysics* 90 (5) 2017: pp. 1213–1218. https://doi.org/10.1007/s10891-017-1676-9